Electronic Supplementary Information for

Vertical SnO_2 Nanosheets@SiC Nanofibers with Hierarchical Architecture for High Performance Gas Sensors

Bing Wang,[a] Yingde Wang,*[,a] Yongpeng Lei,*[,b] Song Xie,[a] Nan Wu,[a] Yanzi Gou,[a] Cheng Han,[a] Qi Shi[a] and Dong Fang [c]

[a]Science and Technology on Advanced Ceramic Fibers and Composites Laboratory, National University of Defense Technology, 109 Deya Road, Changsha 410073, PR China

[b]College of Basic Education, National University of Defense Technology, Changsha 410073, PR China

[c]College of Materials Science and Engineering, Wuhan Textile University, Wuhan 430074, PR China

1. Supplemental Figures and Tables

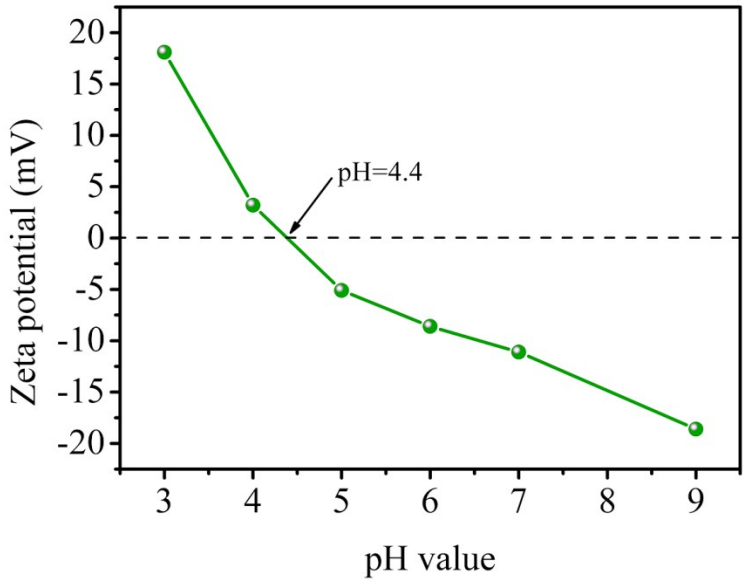

Fig. S1 The pH-dependent zeta-potential curve of SnO_2 NSs@SiC NFs.

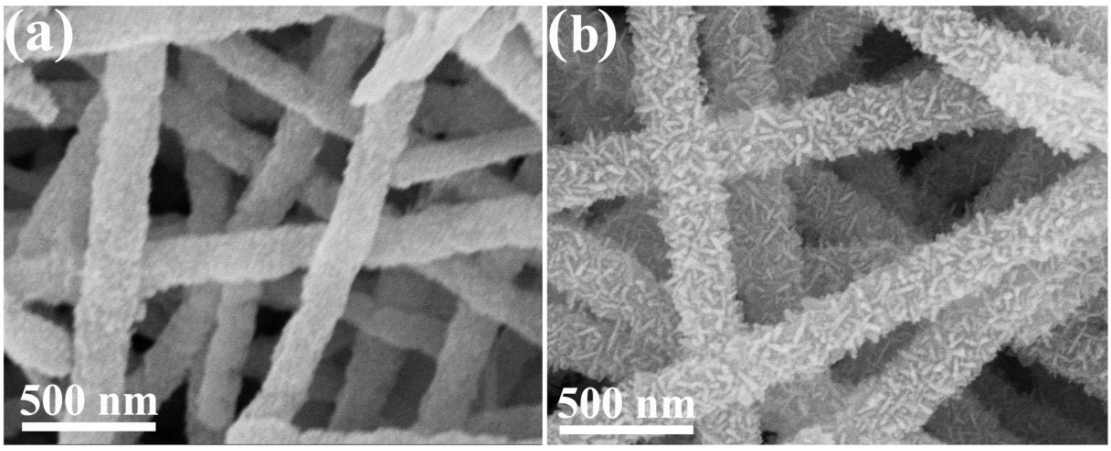

Fig. S2. SnO_2/SiC composite nanofibers synthesized at the hydrothermal reaction temperature of (a) 100 and (b) 160 °C. At the temperature of 100 °C, SnO_2 nanoparticles were grown on the SiC NFs while nanorod-like SnO_2 was observed at the higher temperature of 160 °C.

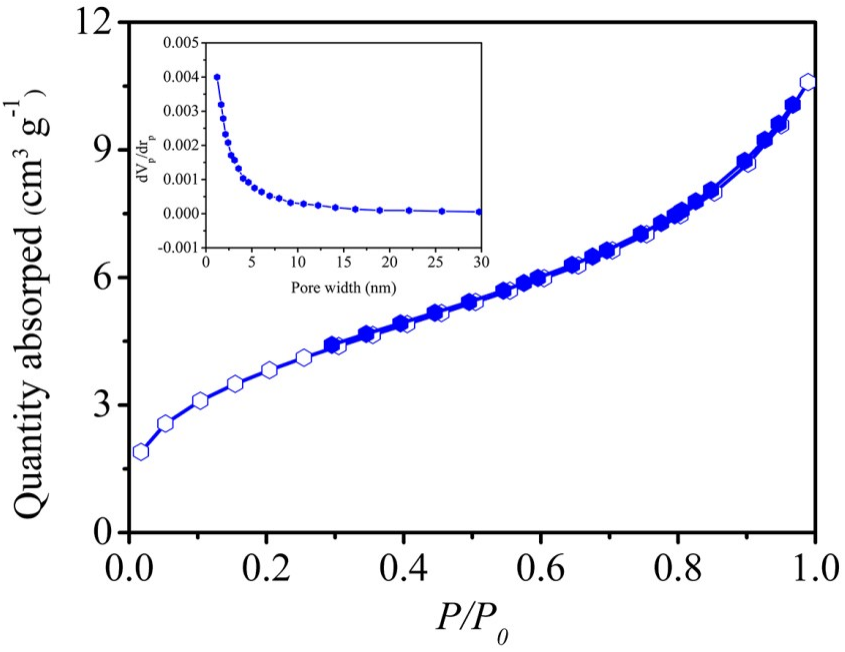

Fig. S3 N_2 adsorption-desorption isotherm of pure SnO_2 NSs. The inset is the corresponding pore size distribution.

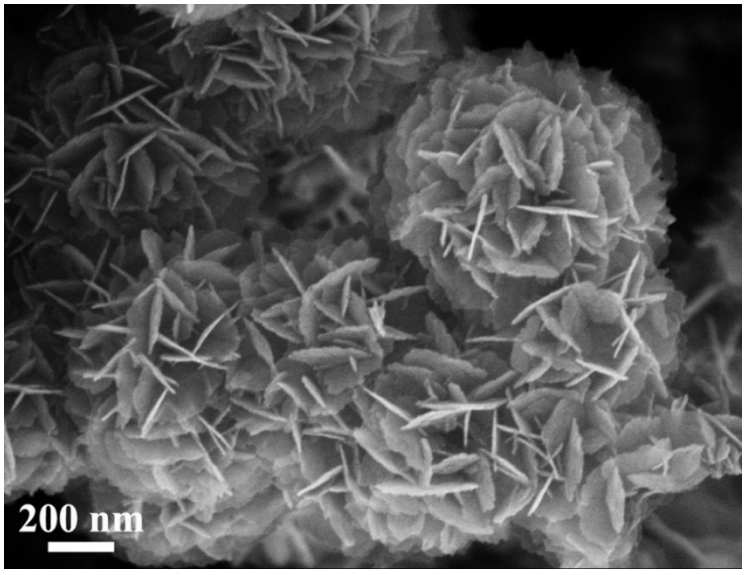

Fig. S4. SEM images of the pure SnO_2 NSs. It is obvious that the SnO_2 NSs aggregates together, lowing the effective sensing area and retarding the desorption of the gas molecules, further leading to the lower sensitivity and slow recovery rate.

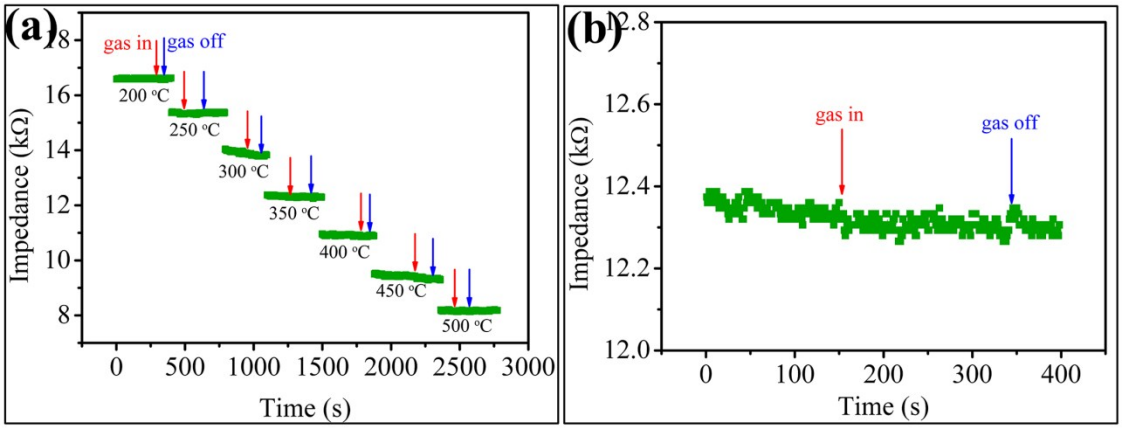

Fig. S5. (a) Gas sensing performance of pure SiC NFs sensor towards ethanol gas from 200 to 500 °C and (b) enlarged view at the temperature of 350 °C.

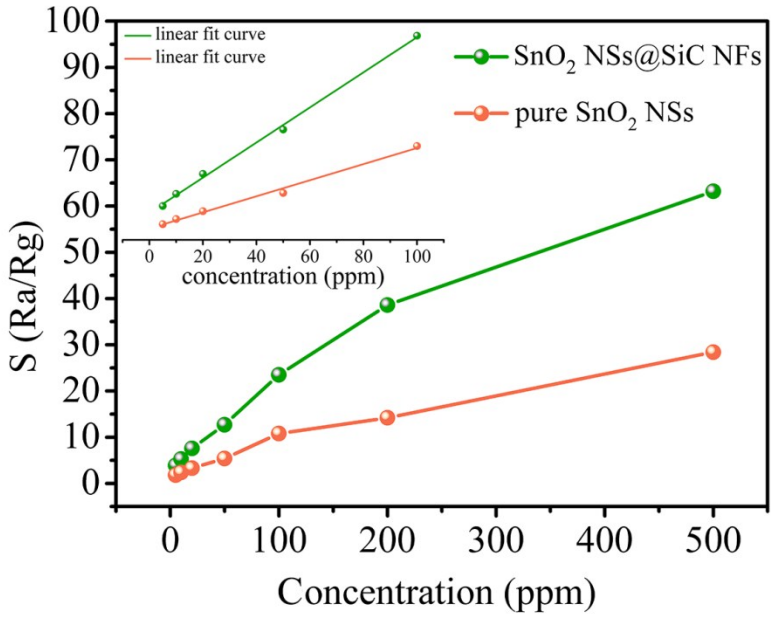

Fig. S6. The sensitivity of SnO_2 NSs@SiC NFs sensor as a function of the ethanol concentration. Inset is the enlarged view at the concentration range of 5-100 ppm . It can be seen that the sensitivity is almost linearly increases with the increasing ethanol concentration, particularly at the concentration lower than 100 ppm.

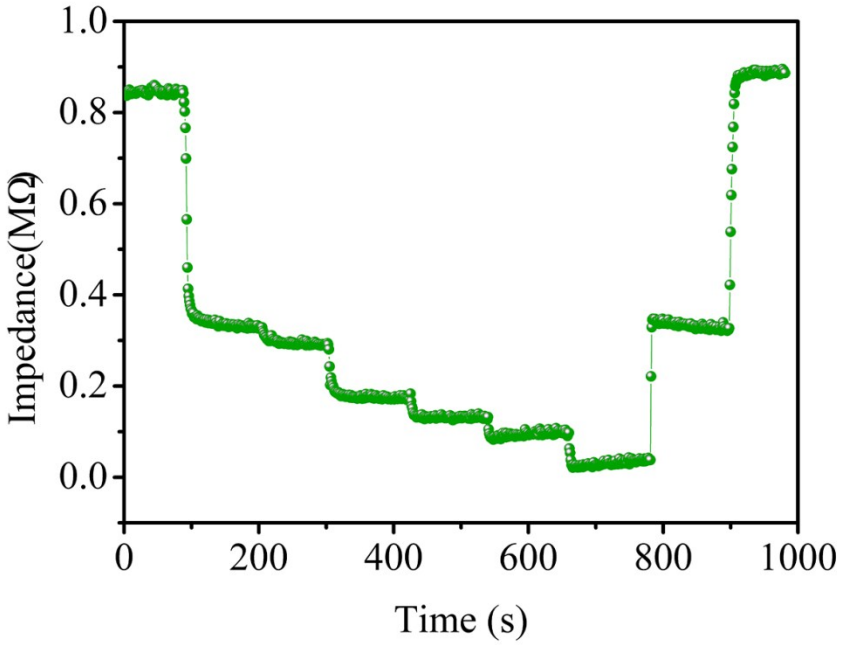

Fig. S7. Dynamic sensing response of the SnO_2 NSs@SiC NFs sensor toward various ethanol concentrations at the temperature of 500 °C.

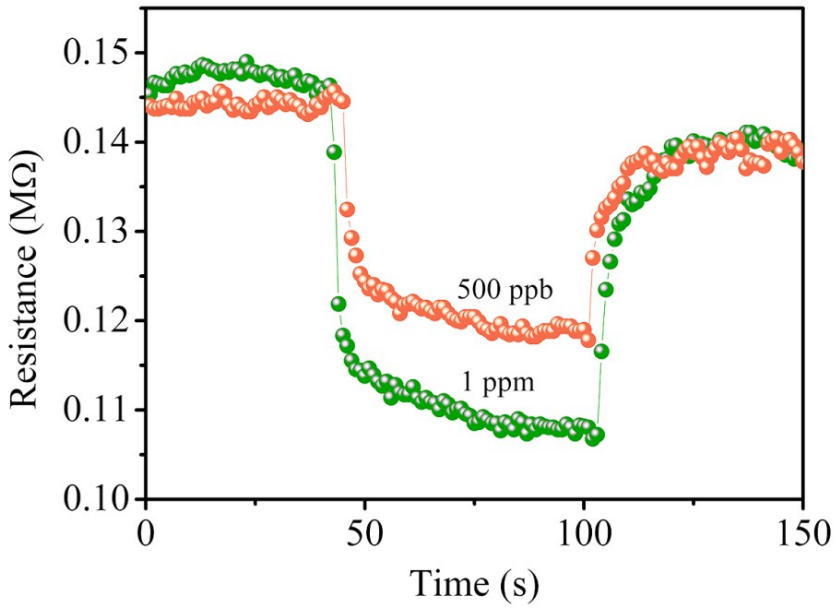

Fig. S8 The response/recovery behavior of SnO_2 NSs@SiC NFs sensor toward 1 ppm and 500 ppb ethanol gas at 350 °C. The responses of sensor are measured to be 1.35 and 1.22 toward 1 ppm and 500 ppb ethanol, respectively， revealing the low detection limit of the SnO_2 NSs@SiC NFs sensor.

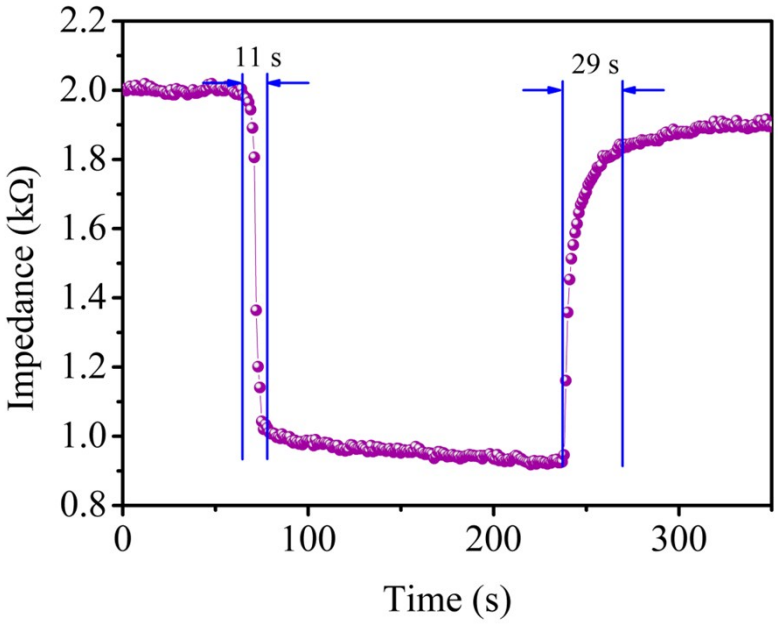

Fig. S9. Response and recovery characteristics of the commercial SnO_2 powders towards 100 ppm ethanol at the temperature of 500 °C.

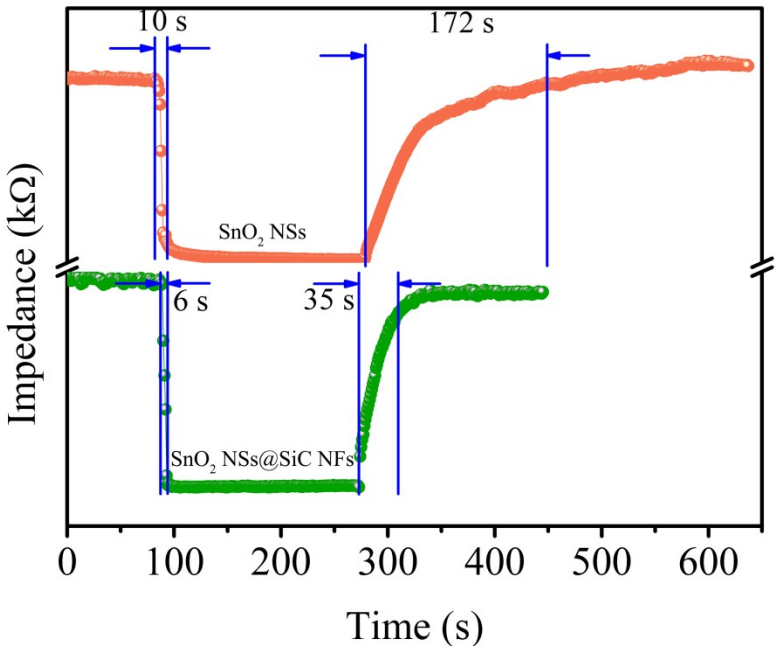

Fig. S10. Response/recovery characteristics of the pure SnO_2 NSs and SnO_2 NSs@SiC NFs sensors towards 100 ppm ethanol at the optimized temperature of 350 °C.

Table S1 Response/recovery behavior of the SnO_2 based gas sensor towards various target gases.

Materials	Target gas	Concentra-tion (ppm)	Operating temperature (°C)	Response/Recovery time (s)
SnO_2-ZnO nanofibers [1]	hydrogen	10	300	187/592
ZnO-SnO_2 [2]	hydrogen	10000	150	60/75
Fe_2O_3@SnO_2 nanotubes [3]	acetone	10	300	5.9/19.8
SnO_2 polyhedrons [4]	acetone	200	370	9.3/5.8
ZnO-SnO_2 nanofibers [5]	Ethanol	100	200	74/12
	acetone	100		111/11
Fe_2O_3/SnO_2 nanotubes [6]	Ethanol	100	200	3/14
	acetone	100		4/12
SnO_2 nanofibers [7]	ethanol	10;50	330	13/13.9 30/-
Hierarchical Zn-SnO_2 nanosheets [8]	ethanol	100	320	14/25
SnO_2/ZnO hierarchical nanostructures [9]	ethanol	100	400	>10s/>15s
In_2O_3-SnO_2 nanofibers [10]	methanol	100	280	8/15
SnO_2 nanorods [11]	isopropanol	100	255	4/10
SnO_2-MCNTs [12]	xylene	3.6	380	>100/>100
SnO_2 NSs@SiC NFs (our work)	ethanol; methanol; isopropanol; acetone; hydrogen; xylene	100; 100; 100; 100; 100; 100;	500; 500; 500; 500; 500; 500;	4/6; 3/9; 3/13; 4/7; 1/15; 5/10;

References

[1] A. Katoch, J. H. Kim, Y. J. Kwon, H. W. Kim and S. S. Kim. *ACS Appl. Mater. Interfaces*, 2015, **7**, 11351-11358.

[2] B. Mondal, B. Basumatari, J. Das, C. Roychaudhury, H. Saha and N. Mukherjee,

Sens. Actuators B, 2014, **194**, 389-396.

[3] Q. Yu, J. Zhu, Z. Xu and X. Huang, *Sens. Actuators, B*, 2015, **213**, 27-34.

[4] D. Chen, J. Xu, Z. Xie and G. Shen, *ACS Appl. Mater. Interfaces*, 2011, **3**, 2112-2117.

[5] W. Li, S. Ma, Y. Li, G. Yang, Y. Mao, J. Luo, D. Gengzang, X. Xu and S. Yan, *Sens. Actuators, B*, 2015, **211**, 392-402.

[6] C. Zhao, W. Hu, Z. Zhang, J. Zhou, X. Pan and E. Xie, *Sens. Actuators, B*, 2014, **195**, 486-493.

[7] Y. Zhang, X. He, J. Li, Z. Miao and F. Huang, *Sens. Actuators, B*, 2008, **132**, 67-73.

[8] Q. Zhao, D. Ju, X. Deng, J. Huang, B. Cao and X. Xu, *Sci. Rep.*, 2015, **5**, 7874.

[9] N. D. Khoang, D. D. Trung, N. V. Duy, N. D. Hoa and N. V. Hieu, *Sens. Actuators, B*, 2012, **174**, 594-601.

[10] W. Zheng, X. Lu, W. Wang, B. Dong, H. Zhang, Z. Wang, X. Xu and C. Wang, *J. Am. Ceram. Soc.*, 2010, **93**, 15-17.

[11] D. Hu, B. Han, S. Deng, Z. Feng and Y. Wang, *J. Phys. Chem. C*, 2014, **118**, 9832-9840.

[12] K. Y. Choi, J. S. Park, K. B. Park, H. J. Kim, H. D. Park and S. D. Kim, *Sens. Actuators, B*, 2010, **150**, 65-72.